UDC 69.04

THE BEHAVIOR OF REINFORCED CONCRETE SLABS ON BASES SUBJECTED TO SHRINKAGE AND CONSTRUCTED WITH COMPLEX HOLE GEOMETRIES

Nan Mou[1], A. E. Zheltkovich[2]

[1] Graduate student, Brest State Technical University, Shandong Huayu University of Technology, Brest – Dezhou, Belarus – China, e-mail: chenchenzi@mail.ru

[2] Candidate of Technical Sciences, Associate Professor, Associate Professor of the Department of Theoretical and Applied Mechanics, Brest State Technical University, Brest, Belarus, e-mail: gelpek@mail.ru

Abstract

This paper presents a comprehensive study on shrinkage cracking in large-scale concrete slabs with complex openings, a critical concern for industrial and civil structures like nuclear plant foundations and industrial floors. The research systematically quantifies the influence of key geometric parameters – hole shape (circular, elliptical, hexagonal) and spatial distribution (centrally symmetric, eccentric, random multi-hole patterns) – on the shrinkage interaction between the slab and its foundation. An integrated methodology combining full-scale experimental testing on 4 × 4 × 0,25 m slabs, theoretical modeling using an enhanced Pasternak – Vlasov foundation model, and detailed finite element analysis (FEA) in Abaqus was employed. Results demonstrate that elliptical holes induce the most severe stress concentration, increasing shrinkage stress by approximately 33 % compared to circular holes, while random multi-hole configurations raise corner stresses by 42 % due to global stiffness reduction. Eccentricity was found to linearly shift the zero-shear stress location (Δx = 0,75 e). A novel predictive model for the stress concentration factor (Kt), incorporating shape aspect ratio (λ), relative eccentricity (e/l), and number of holes (n), was developed with high accuracy (R^2 = 0,92). The study provides essential parameters and robust theoretical support, leading to practical design recommendations for reinforcement detailing and hole geometry optimization to enhance crack resistance in perforated slabs, thereby enabling more reliable and economical engineering solutions.

Keywords: concrete large slabs, complex holes, geometric parameters, shrinkage stress, interaction.

ПОВЕДЕНИЕ ЖЕЛЕЗОБЕТОННЫХ ПЛИТ НА ОСНОВАНИИ ПОДВЕРЖЕННЫХ УСАДКЕ И ВЫПОЛНЕННЫХ СО СЛОЖНОЙ ГЕОМЕТРИЕЙ ОТВЕРСТИЙ

Нань Моу, А. Е. Желткович

Реферат

В данной статье представлено всестороннее исследование усадочных трещин в крупногабаритных бетонных плитах со сложными отверстиями, что является критически важной проблемой для промышленных и гражданских сооружений, таких как фундаменты атомных электростанций и промышленные полы. В ходе исследования систематически количественно оценивается влияние ключевых геометрических параметров – формы отверстий (круглая, эллиптическая, шестиугольная) и пространственного распределения (центрально-симметричное, эксцентричное, случайное расположение нескольких отверстий) – на усадочное взаимодействие между плитой и ее фундаментом. Была использована интегрированная методология, сочетающая полномасштабные экспериментальные испытания плит размером 4 × 4 × 0,25 м, теоретическое моделирование с использованием усовершенствованной модели фундамента Пастернака – Власова и детальный анализ методом конечных элементов (FEA) в Abaqus. Результаты показывают, что эллиптические отверстия вызывают наиболее сильную концентрацию напряжений, увеличивая усадочные напряжения примерно на 33 % по сравнению с круглыми отверстиями, в то время как случайные конфигурации с несколькими отверстиями повышают угловые напряжения на 42 % из-за общего снижения жесткости. Было обнаружено, что эксцентриситет линейно смещает местоположение нулевого сдвигового напряжения (Δx = 0,75 e). Была разработана новая модель прогнозирования коэффициента концентрации напряжений (Kt), включающая в себя соотношение сторон формы (λ), относительную эксцентриситет (e/l) и количество отверстий (n), с высокой точностью (R^2 = 0,92). Исследование предоставляет важные параметры и надежную теоретическую поддержку, что позволяет сформулировать практические рекомендации по проектированию арматуры и оптимизации геометрии отверстий для повышения сопротивления растрескиванию перфорированных плит, что в свою очередь обеспечивает более надежные и экономичные инженерные решения.

Ключевые слова: большие бетонные плиты, сложные отверстия, геометрические параметры, усадочное напряжение, взаимодействие.

Introduction

Large-scale concrete slabs, such as those employed in nuclear power plant containment foundations and expansive industrial floors, invariably require the incorporation of openings to accommodate essential equipment and service conduits. The introduction of these geometrically complex perforations disrupts the structural continuity and alters the stiffness distribution of the slab. Consequently, under the restraining action of the foundation, shrinkage-induced tensile stresses are not uniformly distributed but instead concentrate at the peripherals of the openings and the corners of the slab. This stress concentration phenomenon significantly elevates the propensity for cracking [9].

Prevailing structural design codes, including GB50010 and ACI318, primarily provide guidance for reinforcement detailing around singular, centrally located circular openings [4, 20]. However, these specifications lack comprehensive provisions for non-circular hole geometries or asymmetric distribution patterns. This regulatory shortfall often leads to inadequate crack control in practical engineering scenarios, as the influence of critical geometric parameters – such as shape, eccentricity, and proximity of multiple holes – is not sufficiently accounted for in the design phase [10]. Consequently, improper consideration of these dimensional attributes is a frequent contributor to cracking failures in actual structures [2].

The phenomenon of shrinkage stress in perforated plates has been the subject of considerable research efforts domestically and internationally [12, 18]. For instance, Kumar et al. determined stress concentration factors for square openings via photoelastic experimentation, reporting values approximately 20 % greater than those for circular holes [11]. A limitation of this work, however, is its omission of other geometrically

complex hole profiles commonly encountered in engineering practice, such as elliptical and hexagonal openings [8]. Subsequent investigations by Zhang et al., utilizing finite element analysis, demonstrated that the presence of eccentric holes alters the distribution of shear stresses, shifting the location of minimum shear within the slab [15]. Notwithstanding this insight, their model did not incorporate the critical parameter of foundation constraint stiffness, which fundamentally governs the slab-foundation interaction [5]. A prevalent gap in the existing literature is the predominant focus on isolated hole typologies, resulting in a lack of systematic comparative analysis across a spectrum of sizes, shapes, and spatial arrangements. Consequently, a significant discrepancy remains between prevailing theoretical models and the complex, multi-variate conditions characteristic of actual engineering applications [16].

To address these research gaps, the present study employs a full-scale experimental approach utilizing large concrete slabs measuring 4 × 4 × 0,25 m. The experimental matrix is designed to systematically investigate three distinct hole shapes – circular, elliptical, and hexagonal – under three distribution patterns: centrally symmetric, eccentric, and random multi-hole configurations. By integrating full-scale testing with theoretical modeling and finite element simulation, this research elucidates the mechanistic influence of complex hole geometric parameters on the shrinkage interaction behavior between the slab and foundation [3]. The ultimate objectives are to establish a practical predictive model for shrinkage stress applicable to engineering design and to provide a robust theoretical basis for the crack-resistant design of perforated slabs.

Materials and Methods

The geometric configuration of openings within a slab is defined by a set of distinct parameters, which are systematically classified in this study into three primary categories: shape, distribution, and quantity.

- The category of Shape Parameters characterizes the cross-sectional geometry of the opening. The investigated shapes:

– are Circular – Defined by its radius, *R*;

– Elliptical – Defined by its major semi-axis *a*, minor semi-axis *b*, and the aspect ratio *λ* = *a*/*b*;

– Regular Hexagonal – Defined by its side length *c*, with an equivalent diameter calculated as *D* = 1,1547*c* for comparative analysis.

- The category of Distribution Parameters describes the spatial arrangement of the hole(s) relative to the slab's centroid:

– Centrally Symmetric: Holes positioned with an eccentricity *e* = 0;

– Eccentric – Holes with a defined offset from the center, within a range of *e* = 0,5–1,5 m;

– Randomly Distributed: Configurations of 3 to 5 holes, whose coordinates (*xi*, *yi*) satisfy the conditions |*xi*|, |*yi*| ≤ 1,8 m and maintain non-overlapping boundaries.

- The category of Quantity Parameters specifies the number of openings present:

– Single hole;

– Double holes, with a center-to-center spacing in the range *s* = 1,0–2,0 m;

– Multiple holes, where the number of holes *n* = 3–5.

A schematic representation illustrating the classification of these complex hole geometric models is provided in Figure 1.

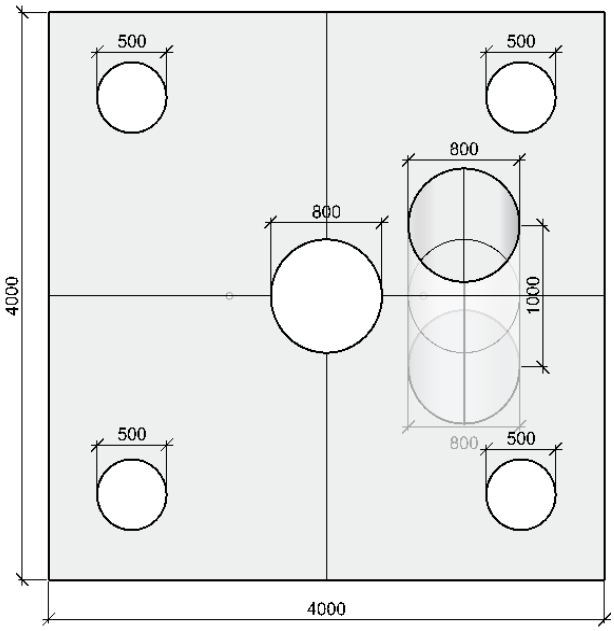

Figure 1 – Schematic diagram of the classification of complex hole geometric parameters

The classical Winkler foundation model, which assumes independent linear springs, is insufficient to capture the shear interaction at the plate-foundation interface, especially when considering the effects of shrinkage and potential shear keys. To account for this, a two-parameter Pasternak – Vlasov model is adopted, which incorporates a shear layer over the Winkler springs. Within the framework of this model, the governing differential equation for the plate with holes, considering shrinkage effects, takes the following form

$$D\nabla^4\omega + K_p\omega = -\alpha T D\nabla^2\omega.$$

Where $= \frac{Eh^3}{12(1-\nu^2)}$, where G is the shear stiffness parameter of the contact layer, K_p is the Winkler foundation modulus, D is the flexural rigidity of the plate, α is the coefficient of thermal expansion, and T represents the shrinkage-induced temperature analog.

For plates with holes, the conformal mapping method using complex variable functions is employed to map the hole region to a unit circle, deriving the expression for the hole edge stress concentration factor Kt

$$Kt = 1 + \beta\sqrt{\frac{k_p l^4}{D}}.$$

Where β is the geometric shape factor: β = 1,0 for circular holes, β = 1,2 + 0,3 ג for elliptical holes, and β = 1,15 + 0,25 n_s (n_s denotes the number of sides) for hexagonal holes [13, 19].

Specimen parameters can be illustrated as follows: six groups of full-scale large slabs (4 × 4 × 0,25 m) were prepared using C30 concrete, each group comprising three hole types, totaling 18 specimens (Table 1).

Table 1 – Experimental working condition design. Compiled by the author

Group	Hole shape	Distribution pattern	Geometric Parameters	Foundation Constraint Stiffness K_p (N/m)
A	Circular	Central symmetry	R = 0,8 m	4 × 10^5 (moderate constraint)
B	Elliptical	Central symmetry	A = 1,2 m, b = 0,6 m (λ = 2:1)	4Ã 10^5
C	Hexagon	Central symmetry	C = 0,7 m (D = 0,8 m)	4Ã 10^5
D	Circular	Eccentric	R = 0,8 m, e = 1,0 m	4Ã 10^5
E	Circular	Random multi-hole	Three holes with R = 0,5 m, randomly distributed	4Ã10^5
F	Elliptical	Eccentric	A = 1,2 m, b = 0,6 m, e = 1,2 m	4Ã 10^5

https://doi.org/10.36773/1818-1112-2025-138-3-41-44

Hole formation. Customized steel molds embedded with PVC pipes (circular), elliptical pipes (major axis parallel to the slab edge), and hexagonal steel pipes were used. The hole walls were coated with a release agent to ensure smoothness, as shown in Figure 2.

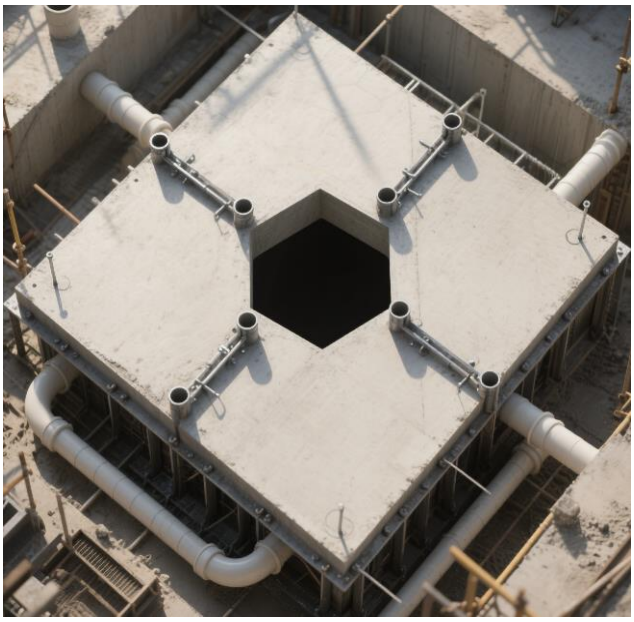

Figure 2 – Schematic diagram of the large slab specimen with hexagonal holes

Shrinkage deformation was quantified using a comprehensive monitoring system. A two-dimensional array of laser displacement meters, configured in a 7 × 7 grid with an inter-node spacing of 0,5 meters, was deployed on the slab surface. This setup was complemented by Digital Image Correlation (DIC) techniques to capture full-field shrinkage strain distributions across the specimen. The combined system achieved a high-resolution measurement capability of 0,001 mm/m for strain [14].

Shrinkage stress within the concrete mass was directly measured using an array of twenty-four embedded Fiber Bragg Grating (FBG) sensors. These sensors were strategically positioned at critical locations, specifically at regions 0,5 meters from hole edges, slab corners, and the central area of the slab, to capture stress concentrations and gradients. Data acquisition was performed at a sampling frequency of 1 Hz, with a measurement accuracy of ± 0,01 MPa [7].

Crack observation was conducted using an automated scanning electron microscope operating at 50× magnification [17]. This instrument was employed to systematically document the precise locations of crack initiation and to trace subsequent propagation paths. The methodology enabled precise quantification of crack widths with an accuracy of 0,005 mm.

A comparative analysis of centrally symmetric hole configurations revealed significant variations in shrinkage stress magnitude. The maximum recorded shrinkage stress at the periphery of elliptical holes (aspect ratio λ = 2:1) reached 3,2 MPa. This value represents a 33 % increase relative to the stress observed at circular holes (2,4 MPa) and a 12,5 % increase compared to hexagonal holes (2,7 MPa). The principal mechanism underlying this stress amplification is the anisotropic stiffness reduction induced by the elliptical geometry [6]. The greater loss of sectional stiffness along the major axis of the ellipse leads to a more pronounced stress concentration at the hole edge compared to the isotropic circular and hexagonal profiles.

The characteristics of stress distribution around the openings were found to be highly dependent on their geometry. For circular holes, the tensile stress field exhibited central symmetry. In contrast, elliptical holes demonstrated distinct stress concentrations, with peak values localized at the terminal points of the major axis. The presence of sharp corners in hexagonal holes resulted in a significant elevation of the stress concentration factor, yielding a Kt value of 2,8, which substantially exceeds the value of 2,0 characteristic of circular openings [1].

The effect of hole eccentricity was pronounced. For a circular hole with an eccentricity (e) of 1,0 m, the maximum tensile stress increased to 2,9 MPa, compared to 2,4 MPa for a centrally located hole. This stress redistribution was accompanied by a lateral shift in the location of zero shear stress by 0,8 m towards the eccentric hole. Analysis confirmed that this shift ($\triangle x$) follows a linear relationship with eccentricity, defined by the function $\triangle x = 0{,}75\ e$.

The introduction of multiple holes in a random distribution further complicated the structural response. Measurements indicated that the stress at the corners of a slab containing three randomly distributed holes was 42 % higher than in an equivalent slab with a single opening. This phenomenon is attributed to a global reduction in slab stiffness caused by the presence of multiple perforations. This stiffness loss triggers a redistribution of in-plane restraint forces, culminating in the formation of new stress concentration zones, particularly in the interstitial regions between the holes (Table 2).

Table 2 – Differences in Crack Propagation Patterns. Compiled by the author

Hole Type	Crack Initiation Location	Propagation Path Characteristics	Critical Cracking Stress (MPa)
Circular Central Hole	Uniform Circumferential Cracking at Hole Edge	Propagation Along 30°–45° Direction from Hole Edge	2.5±0,1
Elliptical Eccentric Hole	Cracking initiates simultaneously at the endpoints of the long axis and at the slab corners	Cracks along the long axis extend toward the foundation edge, while cracks at the slab corners develop at a 45° oblique angle	2,2±0,2
Random multi-hole	Sharp corners at hole edges and weak zones between holes	Inter-hole cracks penetrate, forming a network of cracks	2,0±0,3

Note – Data are derived from 28 days of continuous monitoring; the critical cracking stress corresponds to the stress value at the initial appearance of 0,05 mm cracks.

A three-dimensional finite element model was developed within the Abaqus/Standard environment to simulate the slab-foundation interaction. The concrete slab was discretized using C3D8R elements – eight-node linear brick elements with reduced integration. The foundation restraint was modeled utilizing discrete spring elements, with their stiffness properties defined to reflect the experimental conditions: the horizontal spring constants (K11, K22) were set equal to the foundation constraint stiffness K_p, while the vertical stiffness (K33) was assigned a magnitude of 10K_p to represent the higher resistance to uplift.

The displacement (Δx) calculated using the derived relationship $\Delta x = 0{,}75\ e$ showed a divergence of less than 10 % from the FE simulation results. This close agreement corroborates the postulated influence of geometric parameters on the internal stress equilibrium within the slab.

Through regression analysis, a predictive model for the hole edge stress concentration factor Kt was established

$$Kt = 1.0 + 0.8\lambda + 0.5\frac{e}{l} + 0.3(n-1),$$

where λ is the aspect ratio of the elliptical hole (1,0 for circular holes, 1,15 for hexagonal holes); $\frac{e}{l}$ is the relative eccentricity (l is the half-length of the slab short side, l = 2 m); n is the number of holes.

The model's fit to experimental data is R^2 = 0,92, representing a 60 % improvement in prediction accuracy compared to the simplified code formula (which only considers circular central holes), with errors exceeding 30 %.

Based on the experimental and numerical findings, specific design recommendations are formulated to mitigate shrinkage cracking in perforated slabs. Regarding shape selection, circular openings are preferable for crack-sensitive structures due to their superior stress distribution characteristics. When elliptical holes are necessary, their aspect ratio should be limited to a maximum of 2:1, while hexagonal openings require rounding of sharp corners with a minimum radius of 0,1 m to alleviate stress concentrations. For distribution optimization, the eccentricity of asymmetrically placed holes should not exceed 0,5 l (where l is the half-length of the slab's short side), and the spacing between multiple holes must be at least twice the hole diameter to prevent cumulative stiffness reduction and associated stress amplification.

The reinforcement strategy must be adapted to these geometric parameters. The design of additional circumferential reinforcement at hole edges should be based on the calculated stress concentration factor (K_t). Elliptical holes necessitate a 30 % increase in the reinforcement ratio compared to circular holes, and radial bars (e. g., Φ12@100mm, length 1,0 m) are essential at the vertices of hexagonal openings. Furthermore, slabs with randomly distributed multiple holes require localized strengthening at the corners, achieved by arranging double-layer bidirectional reinforcement (e. g., Φ14@150mm) over a 1,5 m area from each slab corner to resist the significantly elevated tensile stresses identified in such configurations [9].

Conclusion

From the above analysis, it is evident that hole shape (circular/elliptical/hexagonal) and distribution pattern (central symmetry/eccentric/random) both influence the shrinkage stress state of concrete large slabs. Compared to circular holes, elliptical holes exhibit the most severe stress concentration, increasing by approximately 35 %, while random multi-hole slabs cause stress at the slab corners to increase by about 42 %.

A stress concentration factor prediction model based on geometric parameters was developed (R^2 = 0,92), overcoming the limitations of standards that address only single hole shapes and providing quantitative metrics for the design of complex holes.

A targeted reinforcement scheme was proposed to address crack resistance design in concrete structures with asymmetric polygonal holes, maintaining reinforcement errors within 15 % and achieving favorable engineering application outcomes.

References

1. Brouwer, K. J. M. Structural performance of steel-concrete composite floor systems utilising reused concrete slabs / K. J. M. Brouwer // Delft University of Technology. – 2025. – 127 p.
2. Golewski, G. L. The phenomenon of cracking in cement concretes and reinforced concrete structures: the mechanism of cracks formation, causes of their initiation, types and places of occurrence, and methods of detection – a review / G. L. Golewski // Buildings. – 2023. – Vol. 13. – No. 3. – P. 765.
3. Gomes, J. G. Design of reinforced concrete slabs under the combined effect of restrained shrinkage and applied loads : Doctorate Thesis in Civil Engineering / J. G. Gomes. – Braga : Universidade do Minho (Portugal), 2023. – 24 p.
4. Huang, Y. Finite element analysis of the shear performance of reinforced concrete corbels under different design codes / Y. Huang, L. Peng, H. Wei // Buildings. – 2024. – Vol. 14, No. 10. – P. 3100.
5. Long, V. T. Postbuckling responses of porous FGM spherical caps and circular plates including edge constraints and nonlinear three-parameter elastic foundations / V. T. Long, H. V. Tung // Mechanics Based Design of Structures and Machines. – 2023. – Vol. 51, No. 8. – P. 4214–4236.
6. Manohar, R. Influence of Stress-Induced Soil Anisotropy on Geotechnical Design: A Critical View / R. Manohar, S. Saride // Indian Geotechnical Journal. – 2025. – P. 1–19.
7. Moreno, C. The acquisition rate and soundness of a low-cost data acquisition system (LC-DAQ) for high frequency applications / C. Moreno, A. Gonzalez, J. L. Olagotia, J. Vinolas // Sensors. – 2020. – Vol. 20, No. 2. – P. 524.
8. Murru, P. T. Stress concentration due to the presence of a hole within the context of elastic bodies / P. T. Murru, K. R. Rajagopal // Material Design & Processing Communications. – 2021. – Vol. 3, No. 5. – P. E219.
9. State-of-the-art in the mechanistic modeling of the drying of solids: A review of 40 years of progress and perspectives / P. Perré, R. Remond, G. Ameida [et al.] // Drying Technology. – 2023. – Vol. 41, No. 6. – P. 817–842.
10. Barriers, bottlenecks, and challenges in implementing safety I-and safety II-enabled safe systems of working in construction projects: a scoping review / H. Sarvari, D. J. Edwards, I. Rillie, C. Roberts // Buildings. – 2025. – Vol. 15, No. 3. – P. 347.
11. Sharma, K. Nonlinear stability and failure analysis of perforated FGM plate / K. Sharma, D. Kumar // Indian J Pure Appl Phys. – 2016. – Vol. 54, No. 10. – P. 665–675.
12. Study on the wrinkling behavior of perforated metallic plates using uniaxial tensile tests / H. Tang, T. Wen, Y. Zhou [et al.] // Thin-Walled Structures. – 2021. – Vol. 167. – P. 108–132.
13. Timoshenko, S. Theory of Elasticity / S. Timoshenko, J. N. Goodier // New. York McGraw – Hil 1. – 1970. – Vol. 970, No. 4. – P. 279–291.
14. Więch, P. Application of 3D Digital Image Correlation for Development and Validation of FEM Model of Self-Supporting Arch Structures / P. Więch // Advances in Digital Image Correlation (DIC). – 2020. – P. 40.
15. Flexural performance of prefabricated steel-concrete composite beams with post-poured UHPC connections / K. Yu, J. Guo, Z. Zhou, J. Jiang // Structures. – Elsevier, 2025. – Vol. 73. – P. 108–336.
16. Zhang, Y. Effects of Holes and the Confining Pressure on the Mechanical Properties of High-Performance Concrete / Y. Zhang, S. Zhang, Z. Wang // Iranian Journal of Science and Technology, Transactions of Civil Engineering. – 2025. – Vol. 49, No. 3. – P. 2413–2426.
17. Prediction of fatigue crack damage using in-situ scanning electron microscopy and machine learning / J. Zhou, Y. Zhang, N. Wang, W. Gao // International Journal of Fatigue. – 2025. – Vol. 190. – P. 108–637.
18. 带**孔板激光**喷**丸**应**力**传**播及**协调**成形研究** / **李呈**伟 Li Chengwei, **姜高**强 Jiang Gaoqiang, **李**庆佳 Li Qingjia, X. K. Meng // Laser & Optoelectronics Progress. – 2025. – Vol. 62, No. 9. – P. 0914004. – DOI: 10.3788/LOP250429.
19. 赵瑞军. 关于《水运工程混凝土结构设计规范》的建议 / 赵瑞军 // China Harbour Engineering. – 2020. – Vol. 40, No. 6. – P. 39–41.
20. 马福栋, 邓明科, 杨勇. **超高性能混凝土装配整体式框架梁柱**节点抗震性能研究 // [J] **工程力学**. – 2021. – Vol. 38 (10). – P. 90–102. – DOI: 10.6052/j.issn.1000-4750.2020.09.0682. [Fudong, Ma. Seismic experimental study on a uhpc precast monolithic concrete beam-column connection / Ma Fudong, Deng Mingke, Yang Yong // Engineering mechanics. – 2021. – Vol. 38, No. 10. – P. 90–102. – DOI: 10.6052/j.issn.1000-4750.2020.09.0682.]

Material received 04.11.2025, approved 25.11.2025, accepted for publication 26.11.2025